Reduction of thermoelastic noise in gravitational wave antennas by using particular flattened cavity modes

Erika D'Ambrosio

California Institute of Technology, Pasadena 91125 CA

(August 11, 2001)

We explicitly contruct a non-gaussian paraxial cavity mode that has a flat top beam intensity by properly designing the end mirrors of a resonator. The aim is to reduce the thermoelastic noise due to the interaction between the field and the mirror by optimizing the shape of both. We present analytical and numerical results for the spectral density of thermoelastic noise in the special case of a resonator as long as the Fabry-Perot arms of the gravitational wave detector Ligo. We also discuss the alignment stability of such cavity and we mention the most important investigations that are in progress in order to properly design the phase profile of each mirror of the gravitational wave interferometer Ligo. Several numerical simulations have been done in order to understand the impact of a small misalignment in the Fabry-Perot cavity on the power built up inside the arm and the signal picked at the dark port of the beamsplitter. A model for those effects is proposed that takes into account mismatch problems and losses.

INTRODUCTION

In gravitational waves interferometric detectors, the variation of the distance between two mirrors will be measured using the interference between the fields coming out from two perpendicular Fabry-Perot cavities, one of which will sense a squeezing effect while the other will be stretched. Indeed the distance to be measured is between the two reflective surfaces of the mirrors, that are sensed by a field with certain phase and intensity characteristics. We plan to build a Fabry-Perot resonator whose lowest loss mode minimizes the thermoelastic noise. The relevance of this kind of internal thermal noise has been fully understood through mathematical models for both the infinite half-space approximation and finite size mirrors [1–3]. The intensity distribution of the electric field generates a heat flow inside the mirror with temperatures that vary on a small scale, due to the dissipation inside the substrate. If the deposited power were uniform on the mirror's surface the effect would not manifest while for intensity profile with a large gradient the local variations in temperature affect the reflected field because they cause macroscopic distortions due to thermal expansion. When Gaussian fields are used the thermoelastic gravitational wave noise depends on the spot size R_0 and scales as R_0^{-3}. In this context the size of the mirror must be such that diffractional losses are not too high. An optimization for the beam's shape to be as flat as possible with a very small diffractional loss includes a profile that quickly falls down near the edge of the mirror. It must also be a stable mode of the cavity and as well separated by higher order modes as possible. A beam like that is investigated for a cavity as long as the arms of the Ligo gravitational wave antenna. That detector will be described in Sec. I for the case of spherical mirrors. A flat top beam is introduced in Sec. II with the design of the mirrors that can allow that beam to be a stable mode of the cavity. A description of the computation of thermoelastic noise for such field and mirrors is given in Sec. III. The results obtained by using different intensity profiles and different mirrors' forms are quantitatively compared. In Sec. IV we study the sensitivity of the flat top beam to mirrors' misalignment. The details of such analysis are given in Sec. V with the predictions obtained using a second

order approximation in perturbation theory.

In Sec. VI we conclude with some remarks on the increase in sensitivity for the detection of gravitational waves.

I. CONVENTIONAL GRAVITATIONAL WAVE INTERFEROMETER WITH SPHERICAL MIRRORS

Using the following notations:

$$\psi_{ref} = \frac{-r_1 + (r_1^2 + t_1^2)r_2}{1 - r_1 r_2}\psi_{in} = r_{eff}\psi_{in}$$
$$\psi_{tr} = \frac{t_1 t_2}{1 - r_1 r_2}\psi_{in} = t_{eff}\psi_{in}$$

for one Fabry-Perot cavity like the one shown in Fig.1, we can add a recycling mirror and using the coupling between the two cavities we define the effective reflectivity r_{eff} that enters the equation for the power stored inside the recycling cavity

$$\text{Gain}_{r.c.} = t_r^2/(1 - r_r r_{eff})^2$$

according to the scheme of Fig.2. These formulas assume resonance in every cavity, two identical Fabry-Perot arms and an ideal beamsplitter and more complex equations can be written to take into account realistic situations. The interferometer we will focus on is Ligo and we are referring to its design for cavities' lengths and mirrors' diameters. A reduction of thermoelastic noise in spherical mirrors with Gaussian beams is accomplishable by increasing the beam spot size. This must be done taking into account the diffractional losses since the mirrors are finite.

In Fig.3 diffraction losses are shown as a function of the ratio of the mirror radius r and the spot size of the beam w. The values obtained by using two different numerical codes (one based on the FFT of the electric field and one on its decomposition in transverse modes) are ~ 2.5 larger than the naive estimation that evaluates the portion of power lost because of the light clipped outside the border of the mirror. For example if a mirror's diameter of $30cm$ is

taken into account the diffractional loss for a spot size $w = 6.44cm$ is 50 parts per million. A better choice might be a spot size of $6.0cm$ that gives a diffractional loss of $10ppm$. Opting for a conservative choice that is keeping the spherical mirrors gives a constraint on the beam spot size since a diffractional loss larger than $20ppm$ is not acceptable for the advanced Ligo interferometer that is being planned to have Finesse ~ 1250. This goal will not be achieved if power losses are not below the limits fixed by requirements.

II. THE FLAT TOP BEAM AND THE CAVITY WHICH HAS IT AS ITS FUNDAMENTAL MODE

We will overstep the limits put on Gaussian beams by using a non-Gaussian mode. For such field to be an eigenmode of a cavity, the end mirrors must be prepared with a special reflective surface in order to minimize power losses. This means that we are designing the flat top beam in such a way it is a stable mode of a properly chosen cavity. For lengths and mirrors' diameters we will refer to the typical values for Ligo.

Next step is to introduce such mirrors that match with the spatial surface for constant phase of the beam. The kind of beam that was chosen is a superposition of Gaussian profiles whose centers are spread all inside a circle whose radius is ρ. We obtain

$$u(R,\rho) = \int_0^{\rho} \mathrm{d}r \int_0^{2\pi} \mathrm{d}\phi \exp[\frac{2\pi}{\lambda D}(-R^2 + 2\cos\phi Rr - r^2)(1+i)/2] \quad D = \text{cavity length} \quad (1)$$

where the expression $(\vec{R} - \vec{r})^2$ is shown as a function of ϕ. This superposition of Gaussian fields produces a new shaped beam which obviously is a function of the position $\vec{R}$ and the radius of integration ρ. There are a few points worth noting: the first is that the field shows pretty flat in a circle whose radius is ρ. The second is that ρ cannot be chosen too large in order to limit the diffraction losses. This may be assessed evaluating

$$\frac{\int_{R_m}^{\infty} \mathrm{d}R|u(R,\rho)|^2 R}{\int_0^{\infty} \mathrm{d}R|u(R,\rho)|^2 R} = L$$

where R_m is the mirror radius and L the limit for the diffraction loss. It indicates a certain

$\rho(L)$ which limits the flattened region of the beam. If we apply the same procedure for the Gaussian beam we find a limit on the waist.

D is the length of the Fabry-Perot cavity and λ the laser wavelength.

Numerical values are $D = 3999.01m$ and $\lambda = 1.064 \cdot 10^{-6}m$.

Accepting a loss of $21ppm$ per bounce according to the Ligo design means $\rho(L) = 10.4cm$.

Solving for such L

$$\int_{R_m}^{\infty} |\Psi_{Norm}(\frac{R}{R_0})|^2 2\pi R \mathrm{d}R = L \tag{2}$$

gives $R_0 = 4.88cm$ and this fixes the Gaussian field we will use for reference.

The Gaussian field in (2) is supposed to be

$$\Psi_{Norm}(\frac{R}{R_0}) = \frac{1}{\sqrt{\pi R_0^2}} \exp[-\frac{R^2}{2R_0^2} - i\frac{R^2}{2R_0^2}\frac{\frac{\lambda D}{2\pi}}{R_0^2 + \sqrt{R_0^4 - (\frac{\lambda D}{2\pi})^2}}] \tag{3}$$

normalized. The field u_{Norm} is being formed with $\Psi(\frac{|\vec{R}-\vec{r}|}{\sqrt{\frac{\lambda D}{2\pi}}})$ with $\vec{r}$ covering a circle as shown in Fig.6. It is the same field introduced by (1) as a continuous superposition and it is normalized.

Comparing the flat top beam and the Gaussian field having the same diffraction loss the thermoelastic noise can be evaluated for the two solutions. Because of the reduced profile gradient there is an improvement depending on the ratio of the size of the flat region and the Gaussian beam radius.

Let me stress that if two mirrors are planned so that their surface corresponds to the same phase of a propagating beam they form a stationary cavity. In order to check if this may be a good solution for LIGO, I made some preliminary tests using the associated mirror maps, assuming that

$$h[i,j] = \frac{\lambda}{2\pi}\{\Phi[u(0,\rho(L)] - \Phi[u(R[i,j],\rho(L))]\}$$
$$R[i,j] = \frac{S}{N}\sqrt{(i - \frac{N}{2} - \frac{1}{2})^2 + (j - \frac{N}{2} - \frac{1}{2})^2}$$

with the following notations

$$i,j = \text{pixel indexes} \quad S = \text{grid physical size} \quad N = \text{number of pixels}$$

where $R < R_m$. The naive idea is that a path should be subtracted corresponding to the phase difference [5–7].

Moreover a laser beam is to be used to drive such a cavity and we assume it is Gaussian. Other choices could have been made but this showed to be the best one since a mode cleaner with special mirrors should have been planned in order to prepare a non-Gaussian beam that properly match the flat top beam at the front mirror of the cavity.

To understand more deeply how the incoming Gaussian beam can be connected with the superposition shown above, the difference between the two can be calculated using the metric of Hilbert spaces. After normalizing the two state vectors the following quantity is computed

$$S(R_0) = \int |\Psi_{Norm}(\frac{R}{R_0}) - u_{Norm}(R,\rho)|^2 2\pi R \mathrm{d}R \tag{4}$$

for various values of R_0.

The phase of $\Psi(x)$ is chosen in such a way that the smallest cross section of the beam is at a distance $\frac{D}{2}$. In other words we are referring to a symmetrical cavity otherwise an additive degree of freedom should be take into account that is where inside the cavity the field should have a flat wavefront.

In Fig.7 we can observe a minimum corresponding to $R_0 = 6.54cm$. For such values of R_0 the diffractional losses are high and reach $L = 0.26\%$. We will use this beam as the driving field for the Fabry-Perot cavities otherwise a numerical estimation of the diffraction loss would have been needed. For this situation where the laser beam is used for feeding the resonator, we don't need to take care of the complex situation of many field paths interfering. In other words ther is only one bounce of the driving beam on the front mirror. The loss is simply evaluated by using the geometrical approximation while when the beam is considered a cavity mode that approximation is no longer valid as proved by several and different approaches [4].

III. DESCRIPTION OF METHODS FOR OPTIMAL IMPROVEMENT OF THERMOELASTIC NOISE

Richard's file overview.tex

IV. ALIGNMENT STABILITY OF THE RESONATOR BUILT FOR THE FLAT TOP BEAM MODE

In order to study the sensitivity of the cavity with non-spherical mirrors, the external mirror of one cavity of the interferometer has been titled. The design of the model is not the same of Ligo for the absence of the recycling mirror. A set of preliminary runs has been done in order to check that the flat top beam is the field filling out the cavity when stationary conditions are chieved. The wave front matches the reflective surface of the end mirrors and the reduction of the gain compared to the theoretical value calculated from the reflectivity parameters of the mirrors is exactly what we expect because of the discrepancy between the laser field feeding the cavity and the flat top beam. The recycling mirror will be included when the shape of the internal mirror will be designed.

When the light is not made circulate inside the recycling cavity, the symmetric port of the beamsplitter carries the whole field coming out of the Fabry-Perot cavities and reflects it back toward the laser. If an external mirror is tilted a small amount of power is lost through the antisymmetric port since the beams coming out of the cavities are not exactly the same. Moreover part of the power built up inside the long arm cavity is lost because the match with the driving beam gets worse and the portion of the beam entering the cavity decreases. This is clearly shown by the simulation results since the gain of the cavity with a misaligned mirror is reduced while the power in the other one is kept constant.

The diffraction losses vary very slowly and they are not a problem. For example they are increased by $0.05 ppm$ for an angle error of 0.010μrad. The results for the antisymmetric port are shown in Fig.12. The symmetric port power is so close to one that those values are

also the ratio between the two exits of the beamsplitter. A tilt of 0.005μrad gives a value for that ratio corresponding to the limit expected for Ligo that is 10^{-4}. This means that the performance of the designed control on the alignment of mirrors that is currently fixed for tilts of the order of 0.010μrad must be improved with a view to reduce the thermoelastic noise by using flat top beams.

A very intuitive way to think about this is taking into account that for large radii of curvature cavities are very unstable. The mirrors' curvature helps the beam to stay trapped inside the cavity when it bounces between the two mirrors.

The number of bounces depends on the Finesse of the cavity and it represents a sort of decay time.

If the mirrors are very flat the beam escapes earlier from the cavity and this is the cause of the diffraction loss. Moreover the eigenmode of the cavity with misaligned mirrors can have a poorer overlap with the unperturbed mode. This is the cause of a bad cancellation between the fields coming from the Fabry-Perot cavities since the scalar product of those fields is not longer equal to one. A comparison between the flat top mode's sensitivity to mirrors' angle error and the stability of the Gaussian beam when the spherical mirrors planned for Ligo are implemented in the simulation program may be traced by watching the values in Fig.13. The reflectivity parameters are the same and the recycling mirror is not active.

The dark port intensity is one order of magnitude smaller and within the range of tilt shown in the Figure the power inside the arm cavities doesn't decrease.

This means that the diffraction losses are not much affected inside the cavity with a misaligned mirror.

The instability of the flat top beam may be explained by considering that most of its power is contained in a Gaussian beam whose radius of curvature is very large such that the corresponding g factors are very close to one. If we take the basis of modes for those g factors we can build a combination having the intensity profile we want.

An example is shown in Fig.10. The power profile is of the normalized field (using

Laguerre polynomials)

$$\Psi_{Norm}(\frac{R}{R_0})[(1-\epsilon^2/2)L_0(\frac{R}{R_0}) - \frac{\epsilon}{\sqrt{2}}L_1(\frac{R}{R_0})e^{2i\theta_G} - \frac{\epsilon}{\sqrt{2}}L_2(\frac{R}{R_0})e^{4i\theta_G}] \quad (5)$$

where θ_G is the Guoy phase. All geometrical parameters are fixed by the the Gaussian beam having the best overlap with the flat top beam. ϵ is such that the field in (5) has the same Gaussian portion of the flat top beam. As we can predict the wave front of such field at the location of the mirrors is not spherical.

In other words if we want a flattened beam to be a stable mode of a cavity the two end mirrors must match the wave front. Moreover in order to put a threshold on diffractional losses the diameters have also to be properly designed. If the Finesse of the cavity is very high a reasonable limit is few parts per million, like in Ligo interferometers.

In Fig.11 the phase profile is shown for the field (5). The intensity falls down less rapidly than for a Gaussian beam and the discrepancy between such distribution and a Gaussian function is connected with the design of the mirrors' surface that is characterized by a very high rim at the border.

An alternative could be to investigate the use of a single higher order mode. A limit on this is put by diffractional losses since the intensity curve extends on a larger spot.

V. MAIN RESULTS FROM SIMULATIONS

A. Review of the predictions obtained by applying perturbation theory

Richard's Thermoelastic Summary.nb

B. Analysis of the data with a focus on the experimental implications

In this subsection emphasis is placed on understanding the physical content of the output of the simulation runs. Because of the misalignment of the resonator

$$u_0^{'}(\vec{R}) = \alpha_0 u_0(\vec{R}) + \alpha_1 u_1(\vec{R}) + \alpha_2 u_2(\vec{R}) + \ldots \quad (6)$$

will be the new ground eigenmode of the cavity where u_0, u_1 and u_2 are the ground eigenmode of the unperturbed cavity, the first excited solution with a dipolar behaviour, the second excited state with a specular symmetry referred to the axis the tilted mirror is rotated around and so on. Indeed we assume the modes of the resonator with reshaped mirrors are a complete set of orthonormal functions like for spherical mirrors [8]. In both cases the propagation equation is to be solved but the border conditions differ because of the mirrors' surfaces.

u_0 is $u_{Norm}(R,\rho)$ according to the notation of Sec. II. The choice of ρ has been set by fixing the diffraction loss. The evaluation of the u_1 and u_2 components may be done from the simulations' data. The grid of u_0 is known and it has been checked to be the designed one. The component u_1 can be exctracted selecting the dipolar portion of the field. What we are left with is u_2.

From the numerical results:

$$|\alpha_0|^2 = 1 - 5.14211(\frac{\theta}{\mu\text{rad}})^2$$

$$|\alpha_1|^2 = 5.14262(\frac{\theta}{\mu\text{rad}})^2$$

$$|\alpha_2|^2 = 3.1196(\frac{\theta}{\mu\text{rad}})^4$$

where θ is the angle error. Those constants come from minimizing the sum of the squared of deviations of the numerical data from the guess function. The same kind of analysis may be done at the dark port of the beamsplitter where a signal proportional to θ^2 is picked up. Subtracting the odd combination of the field grid in order to reveal its even component, we find that the power which is not carried by the dipolar part of the field is a very small quantity.

In Fig.14 we can see how small is this residual part. After filtering out the dipolar part of the electromagnetic field exiting the dark port, only a small signal is left.

The estimation of α_0 from data is just what is expected. The eigenstate (6) is properly normalized for $|\alpha_0|^2 = 1 - |\alpha_1|^2 \ldots$. A deeper analysis should involve a study of the skewness

and the octupole. With a view to interpret the signal detected at the dark port we should decompose the feeding beam in the basis $\{u_0^{'}, u_1^{'}, u_2^{'}, \ldots\}$. Since the cavity will be tuned to make the lowest loss mode resonate, if the coefficients of such expansion are

$$(\alpha_0^{'}, \alpha_1^{'}, \alpha_2^{'}, \ldots)$$

when the beam is reflected from the Fabry-Perot, there will be a change in sign between the fundamental mode and the higher components and the reflected field can be expressed as

$$(\alpha_0^{'}, -\alpha_1^{'}, -\alpha_2^{'}, \ldots) \qquad .$$

Such beam interferes with the field reflected from the unperturbed Fabry-Perot at the beam-splitter and the antisymmetric combination will go through the dark port toward the photo-detector.

The field at the dark port may be decomposed by a procedure similar to the one described for eq.(6). The power is mostly contained in a dipolar mode

$$P_{dipolar} = 4.81808(\frac{\theta}{\mu\mathrm{rad}})^2$$

$$P_{non-dipolar} = 31.4982(\frac{\theta}{\mu\mathrm{rad}})^4$$

where the former also contains a component in the ground mode since some power has been scattered to higher order mode in you of the two cavities and this is a cause of imbalance between the beams coming from the two Fabry-Perot. Because of the mismatch between the driving beam and the flat top beam, less power than the total is coupled inside the cavities and only that portion senses the tilt.

This is why $P_{dipolar} = \mathcal{C}|\alpha_1|^2(\frac{\theta}{\mu\mathrm{rad}})^2$.

$$|\int \Psi^*_{Norm}(\frac{R}{R_0})u_{Norm}(R,\rho)2\pi R\mathrm{d}R|^2 = 0.943$$

$$\mathcal{C} = 0.937$$

The overlap between the driving beam and the flat top beam may be estimated as a scalar product and its value is consistent with $\mathcal{C}$. An interpretation for $P_{non-dipolar}$ is less

straighforward. The diffraction losses can affect $P_{non-dipolar}$ significantly since that is a very small quantity. The impact of tilt on diffraction losses is shown in Fig.18. The increase due to misalignment is very small

$$L_{diffr} = [21.34 + 748.6(\frac{\theta}{\mu\text{rad}})^2]\, ppm$$

and is responsible for the total loss shown in Fig.19. This effect is an additional cause of imbalance between the arms and it may contribute to the power contained in $P_{non-dipolar}$ at the dark port. A rough estimate without including this effect is

$$\mathcal{C}(|\alpha_1|^4 + |\alpha_1|^2)(\frac{\theta}{\mu\text{rad}})^4 = 27.76(\frac{\theta}{\mu\text{rad}})^4$$

for $P_{non-dipolar}$ while the observed value is a bit larger than this. Since those quantities are very small, a deep analysis of the second order effects is not in our purposes.

VI. REMARKS AND CONCLUSIONS

Several Fortran programs have been written for analysing the maps of the field inside the interferometer and at the external pick-up points when the simulations are run for a misalignment perturbation.

Since the simulation code has been run with non-spherical mirrors and we only know the "ground mode" of the cavity a post-processing procedure has been set upIwhich uses the unperturbed field as a reference and evaluates the perturbed contribution when one mirror is tilted.

Moreover using the fact that the first excited contribution will be dipolar if only on mirror is tilted, it's possible to even disentangle the first and the second order corrections and their weight.

Ten runs were made increasing the tilt of the ETM mirror in the on-line cavity.

The results gave us much perspective on the dark port output.

- When the dipolar component is subtracted the residual power goes $\sim \theta^4$ and all the power is indeed in the dipolar component which goes like θ^2. Those results can be

interpreted by the decomposition of the electric field inside the misaligned cavity mentioned above.

- At the antisymmetric port the excited components are detected since they are not cancelled in the combination with the beam coming from the unperturbed cavity, but also a portion of the ground state beam since its weight IS NOT the same in the two combining beams. In perturbation theory this would be stated as a "normalization condition". What happens is that a portion of the power is moved from the ground state to the higher order modes and that imbalance shows up at the antisymmetric port.

- A slighter effect is due to diffraction losses but they are not significant. They also increase with θ^2 but the increment over the maximum angle error that has been studied that is $10^{-8}\,rad$ is only $5\,10^{-8}$. So the diffraction loss may be considered almost stable around the value fixed as our limit that is 21ppm. Such limit has been mathematically evaluated as the amount of power clipped outside the edge of the mirror. An estimation was done by processing the simulation output and solving the equation for the gain including such internal losses: the same value has been found and this is closely related with the decomposition of the field resonating inside the arm cavity, even when no tilt is active.

Results on thermoelastic noise are given in Richard's manuscript. An evaluation has been made to optimize the Gaussian beam that drives the interferometer. The choice was to maximize the overlap with the flat top beam. That overlap is very good indeed since the squared modulus of the scalar product of those fields is ~ 0.94. In other words most of the flat top beam is contained in a Gaussian whose spot size is $9.25cm$ on both the mirrors of the Fabry-Perot cavities. If a comparison is done with the Ligo II design, which provides a spot size on the mirrors inside the Fabry-Perot cavities of $6cm$ the decrease of thermoelastic

noise should be roughly

$$\frac{S_{flat-top}}{S_{LigoII}} = (\frac{6.0}{9.25})^3 = 0.27$$

by simply applying the scaling law from the expression for thermoelastic noise.

As a consequence of this crude approximation the improvement in sensitivity of gravitational wave detectors is

$$\frac{h_{flat-top}}{h_{LigoII}} = \sqrt{0.27} = 0.52 \qquad .$$

---

[1] F. Bondu, P. Hello, J. Y. Vinet *Phys. Lett. A* 246 (1998)

[2] V. B. Braginsky, M. L. Gorodetsky, S. P. Vyatchanin *Phys. Lett. A* 264 (1999)

[3] Y. T. Liu, K. S. Thorne *Phys. Rev. D* 15 (2000)

[4] We thank Robert Spero for having outlined this issue with private communications.

[5] P. A. Belánger, C. Paré *Opt. Lett.* Vol.16 N.14 (1991)

[6] P. A. Belánger, R. L. Lachance, C. Paré *Opt. Lett.* Vol.17 N.10 (1992)

[7] P. A. Belánger, C. Paré *IEEE Journal of Quantum Electr.* Vol.28 N.1 (1992)

[8] H. Kogelnik, T. Li *Applied Optics* Vol.5 N.10 (1966)

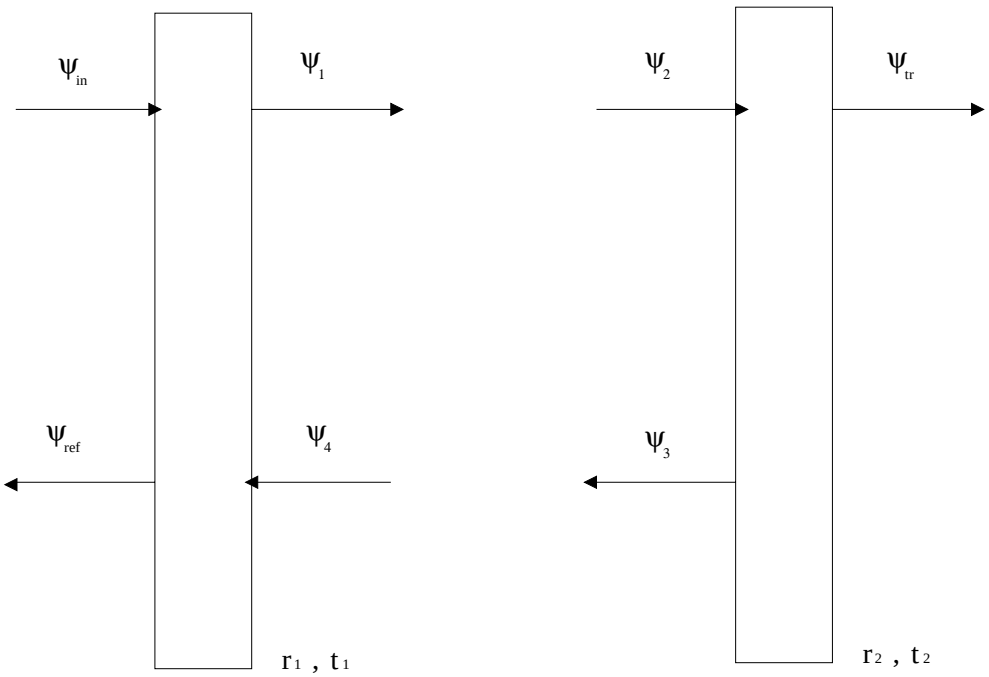

FIG. 1. Schematic of a Fabry-Perot arm cavity with the internal and the external mirrors put according to our notation at the left and right end of it

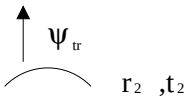

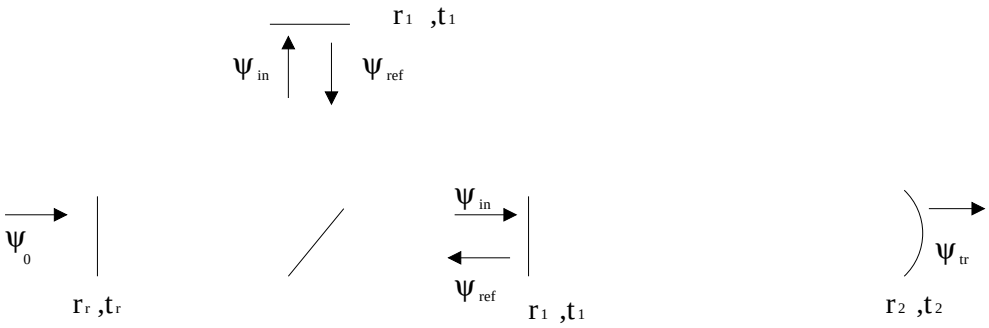

FIG. 2. The arm cavities and the recycling cavity

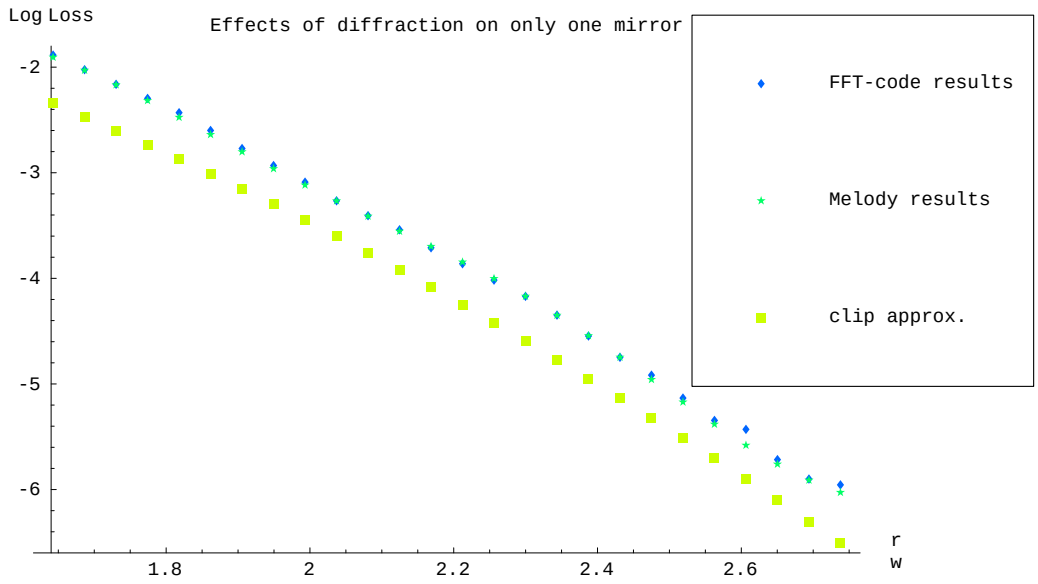

FIG. 3. Three sets of diffractional losses: two of them are obtained by numerical codes and one is calculated by the light falling outside the edge of the mirror (clip approximation)

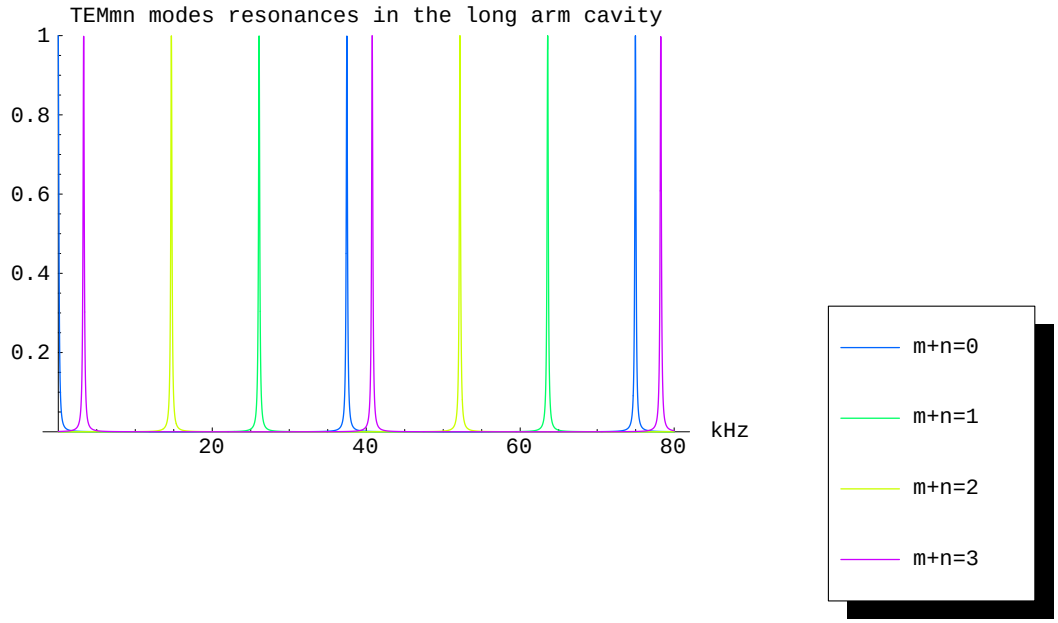

FIG. 4. The operating characteristics of Ligo interferometer are listed in the document LIGO-T970122-00. The free spectral range of the two Fabry-Perot arms is $37.5kHz$ and the Guoy frequency shift is $11.4kHz$. The resoluation of a fringe is $181Hz$. This means that accidental coincidences between resonances are avoided at least for the first higher order modes like the ones shown here

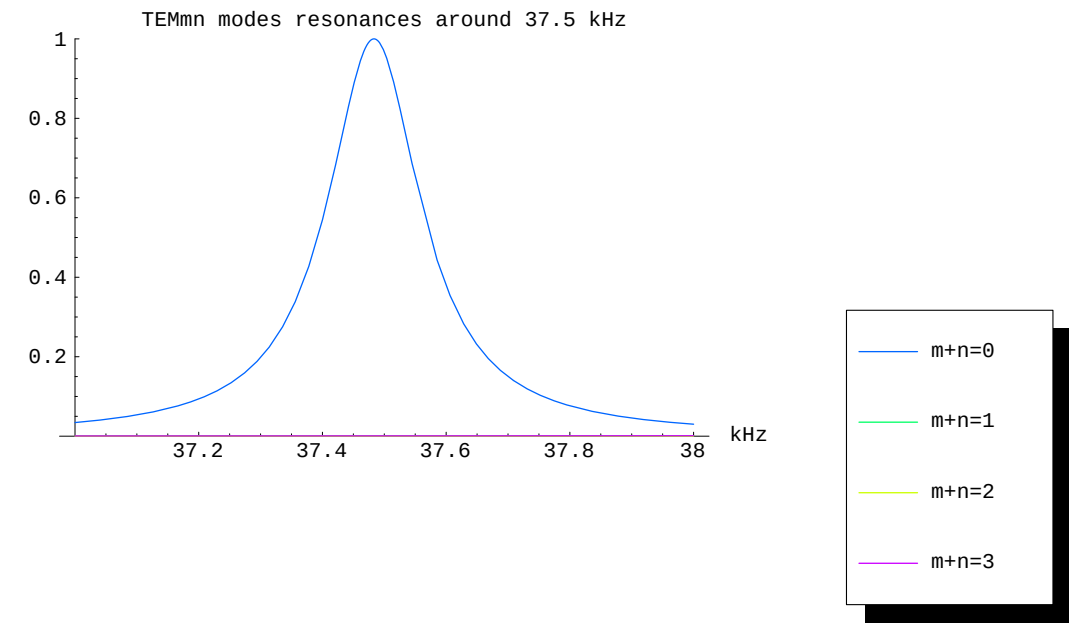

FIG. 5. The width of the resonance peak is small because of the Finesse of the Fabry-Perot that is very high. The fundamental mode and the higher order modes do not overlap

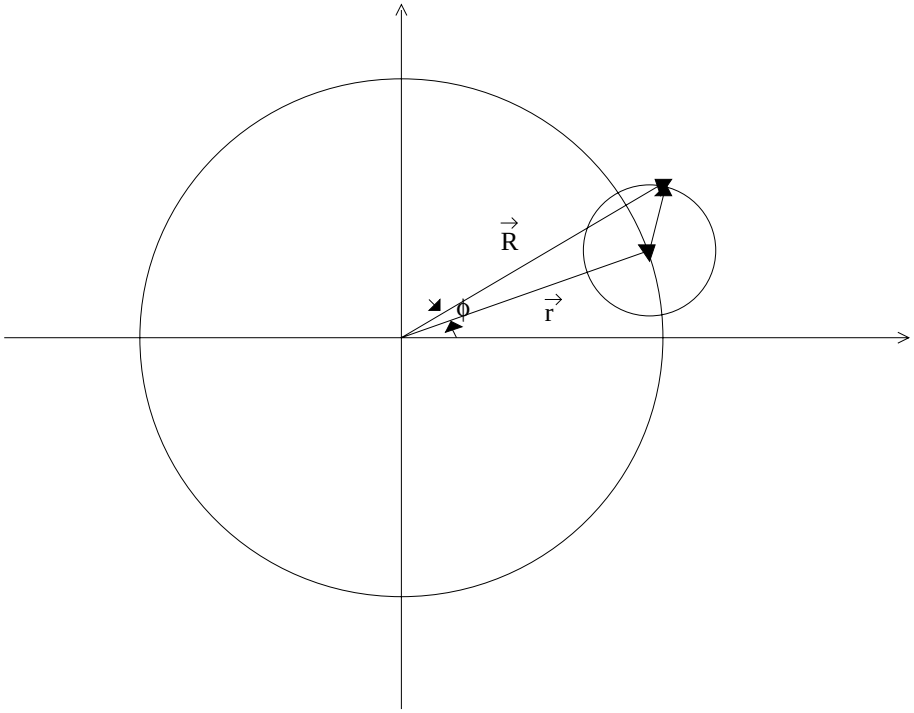

FIG. 6. Superposition of Gaussian fields whose centers are in $\vec{r}$, where of course $0 < |\vec{r}| < \rho$ and $\rho < R_m$. Indeed $\rho = \rho(L)$ and L is the diffraction loss limit which is going to be fixed as $21ppm$ per bounce. This will mean $\rho = 10.4cm$

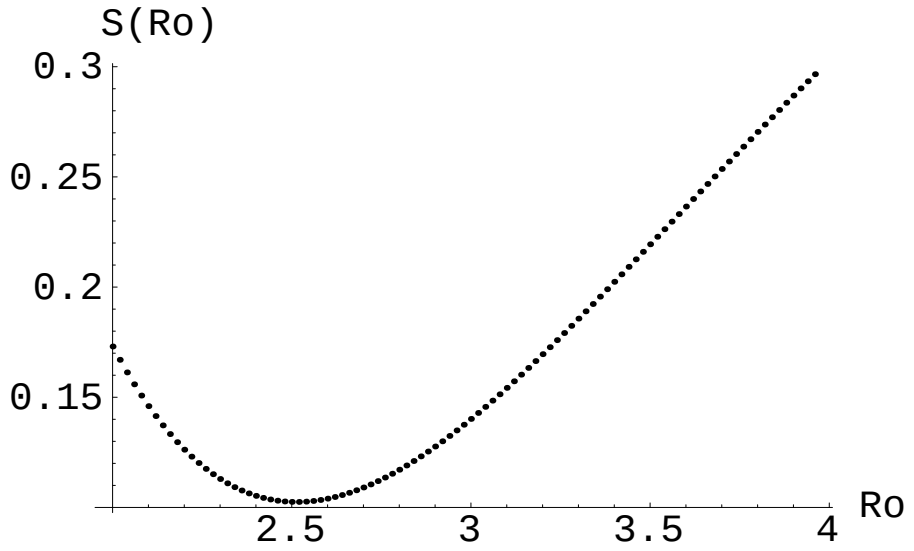

FIG. 7. Minimization of the vector difference between the Gaussian beam state and the superposition mode. The x-axis for R_0 is expressed in units of $\sqrt{\frac{\lambda D}{2\pi}}$. The loss L for the Gaussian beam having radius $R_0 = 6.54cm$ corresponding to the slightest $S(R_0)$ turns out to be $2600ppm$

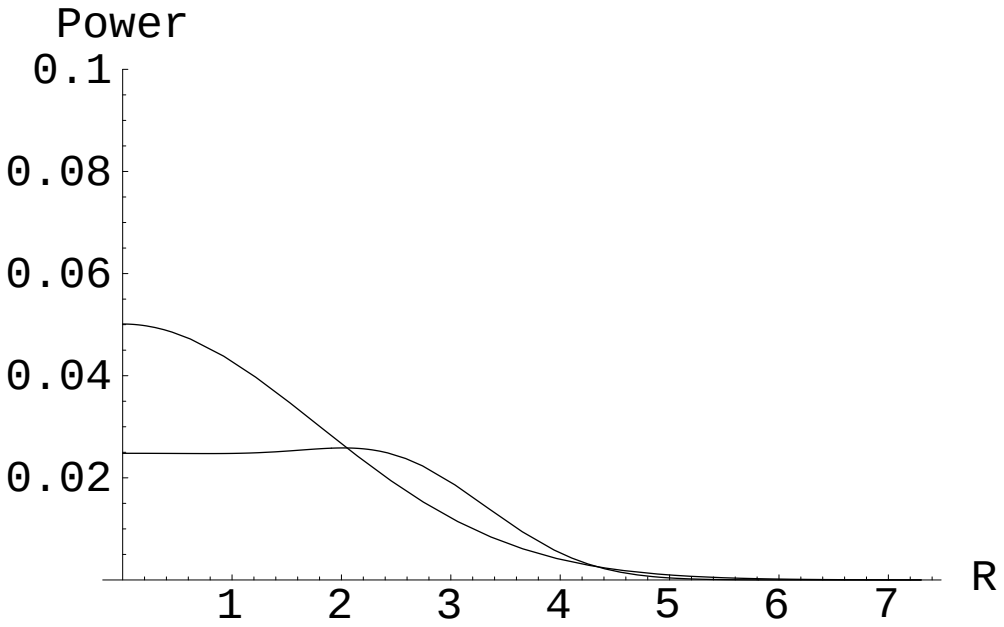

FIG. 8. The power distribution of the flat topped mode and the Gaussian one with $R_0 = 6.54cm$. The x-axis is in units of $\sqrt{\frac{\lambda D}{2\pi}}$

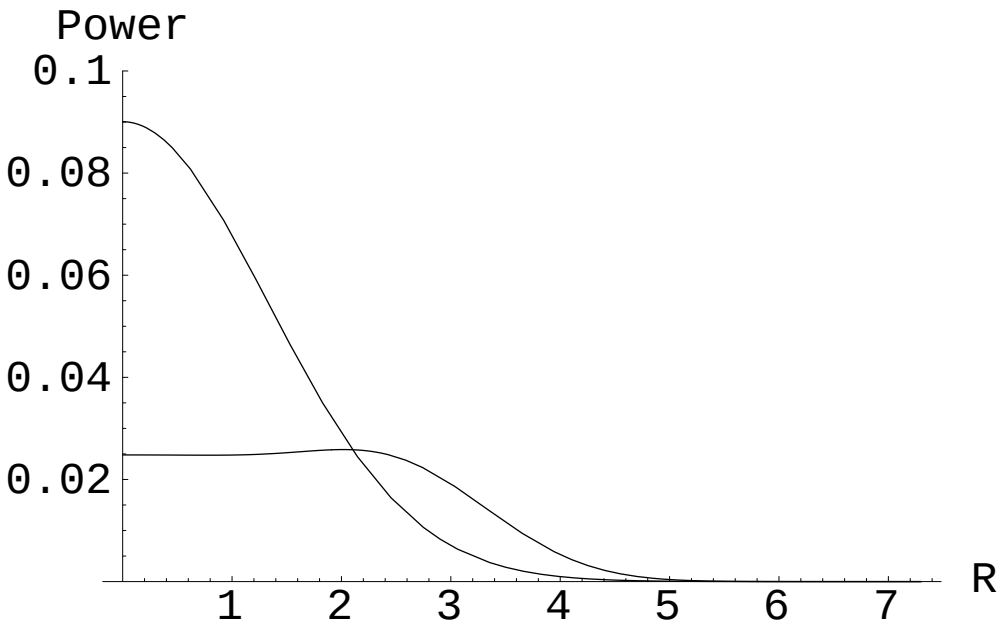

FIG. 9. The power distribution of the flat topped mode and the Gaussian one having same loss $L = 21ppm$ which means a Gaussian beam radius $R_0 = 4.88cm$

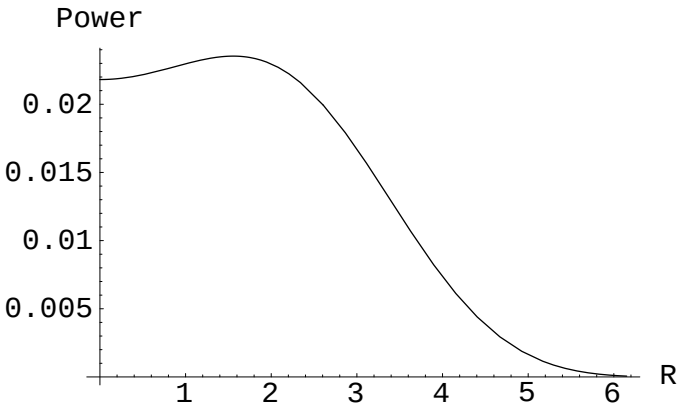

FIG. 10. The intensity profile is shown for a field constructed by using a combination of modes. The basis is defined by the eigenmodes of a cavity with spherical mirrors and the result is not the eigenmode of that cavity since the wavefront of this field doesn't match the spherical surface of the end mirrors

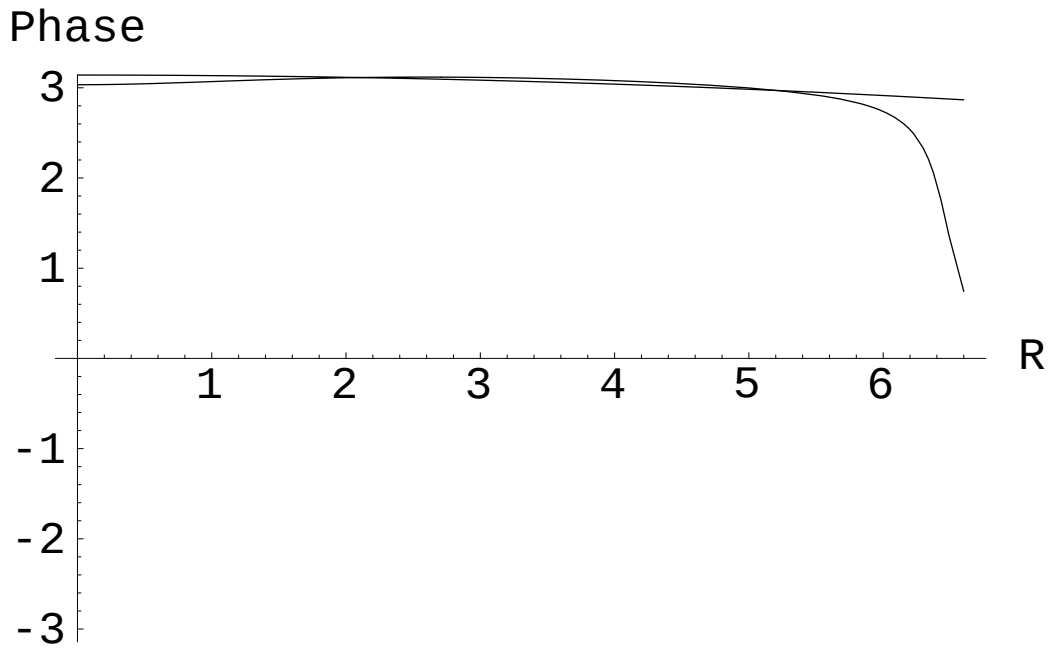

FIG. 11. The spherical phase of the lowest loss eigenmode of a resonator with conventional mirrors is plotted together with the wave front of the field obtained by a combination of eigenmodes of that cavity. Though the contribution of higher order modes is $\sim 10\%$ in terms of power the combination of modes has a wave front at the mirrors location showing a large perturbation far from the central area. To make this field a stable solution the phase surface of the mirrors should match the wave front and the size should be designed by putting a limit on diffraction losses. Since the intensity profile is pretty flat large mirrors are necessary for limiting the amount of light that misses the surface

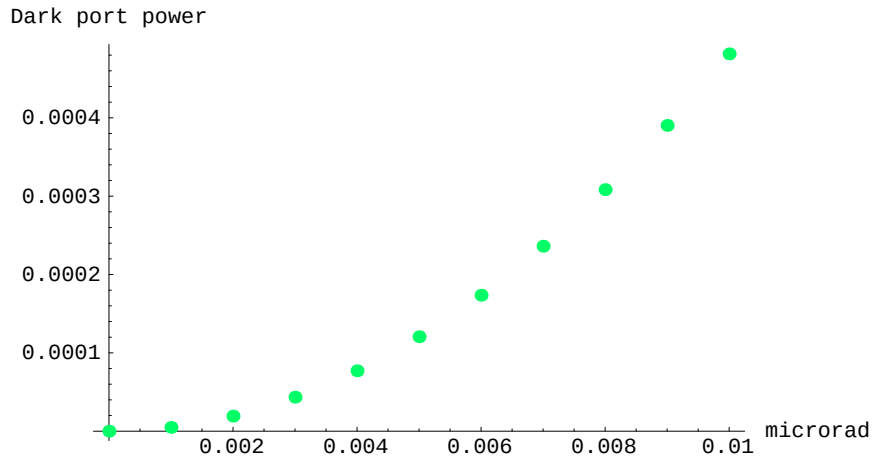

FIG. 12. This plot shows the impact on the symmetry of the configuration when the front mirror of one Fabry-Perot cavity only is titled. The bright port of the beamsplitter decreases of 0.0005 on the same range. The laser power is $1W$ so that the output numbers of the simulation are automatically normalized

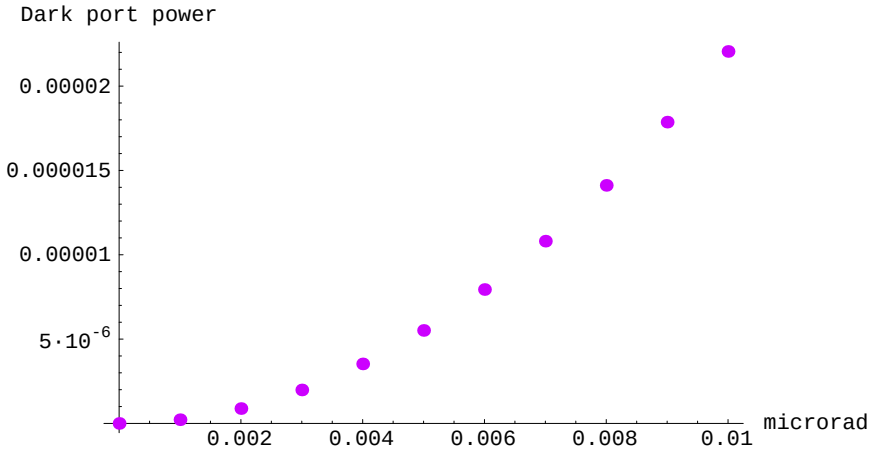

FIG. 13. The dark port of the beamsplitter is far smaller in the case of spherical mirrors than it is when non-spherical mirrors are used. The runs have been performed with no power recycling and using the same Finesse for the arms as in the simulations of the interferometer when the flat top beam was excited

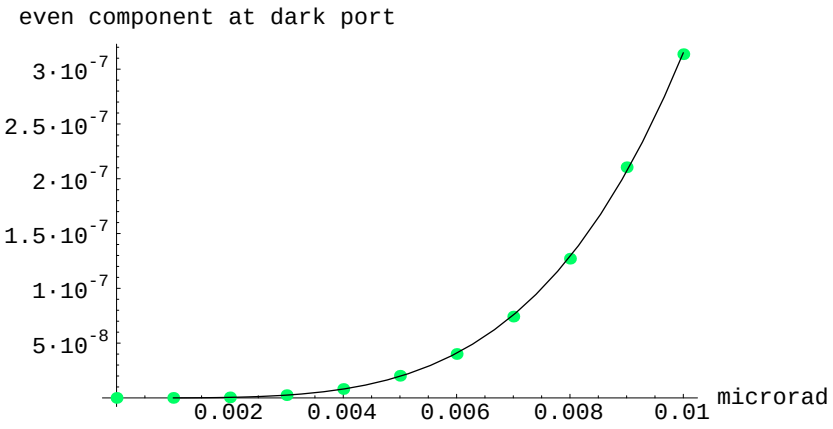

FIG. 14. The power associated with the even component of the field going out of the anti-symmetric port as a function of the angle error of the external test mass mirror. The fit curve $31.5(\frac{\theta}{\mu\text{rad}})^4$ is shown and the agreement with the numerical results is pretty good. Since the tilt has a first order effect on an odd excitation of the field, the noise associated to that may be filtered out without affecting the gravitational wave signal. Using a mode-cleaner at the antisymmetric port will cut down the power due to a tilt

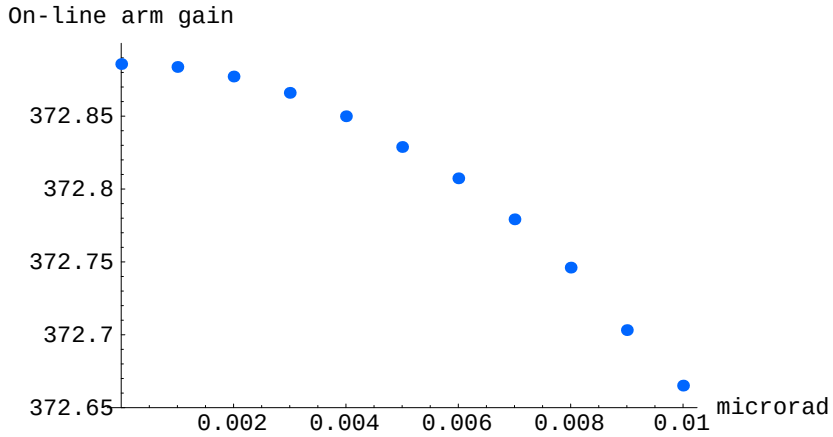

FIG. 15. As expected the power inside the misaligned cavity decreases as a quadratic curve depending on the angle error. The line represents the fit and the points are the values obtained by the runs for $1W$ of laser power. This is the impact of a slight misalignement on the performance of the resonator built by non-spherical mirrors. No decrease is appreciated in the other cavity of the interferometer having aligned mirrors

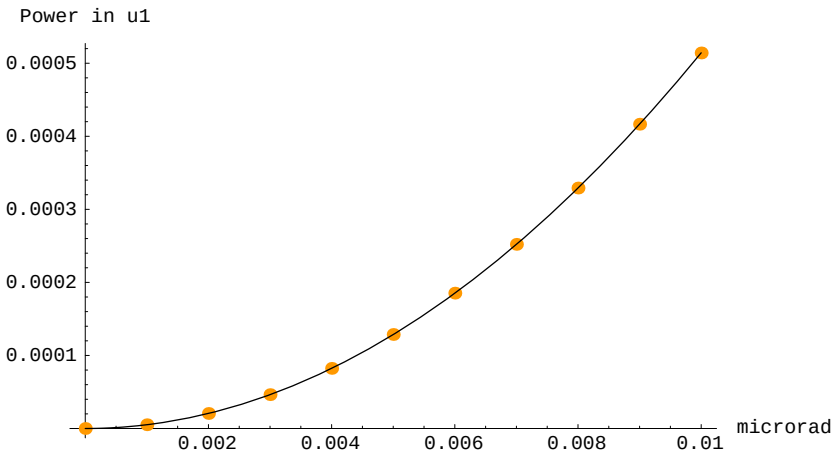

FIG. 16. Results of the evaluation of the portion of power due to higher order modes when the cavity is misaligned. The contribution of the first higher order mode is dominating

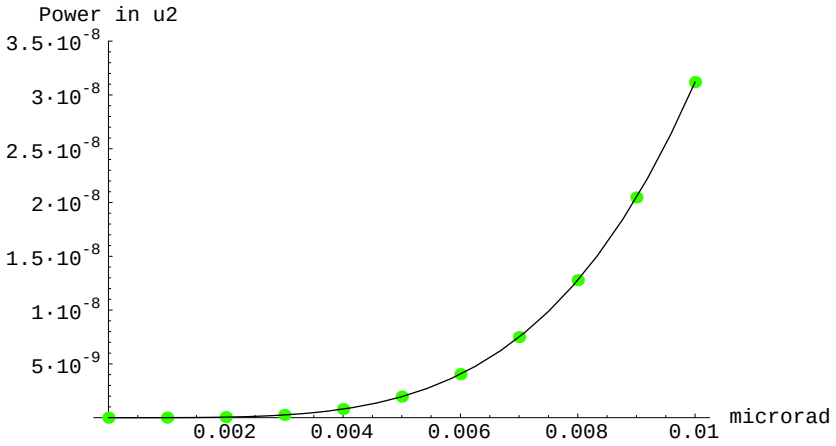

FIG. 17. Only a small portion of the power is contributed by non-dipolar modes. From this graph and the previous one an estimation of $|\alpha_2|^2$ and $|\alpha_1|^2$ is obtained. Those quantities are related with the expression of the field as a perturbative expansion in terms of the modes of the unperturbed cavity and follow the notations of (6). The associated field u_2 is even for reflection across the axis the titled mirror is rotated around, and it contains a purely radial component. These data have been obtained by applying a decomposition algorithm to the grid representing the electric field inside the cavity. Those grids are the output of a numerical program using which the whole interferometer may be simulated

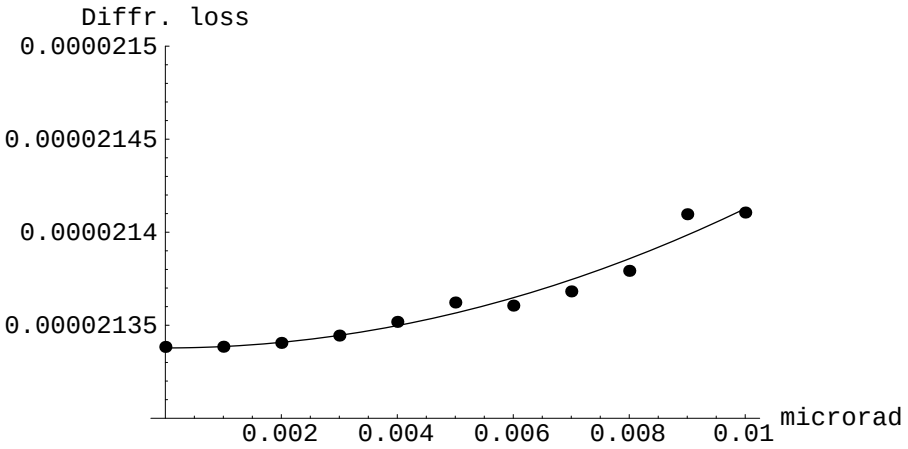

FIG. 18. Diffraction losses in the misaligned cavity. They are estimated by solving the equation for the gain inside the cavity, taking into account the unknown losses and the mismatch between the driving beam and the field excited inside the cavity, for the value observed as a result of the simulation program used for these studies

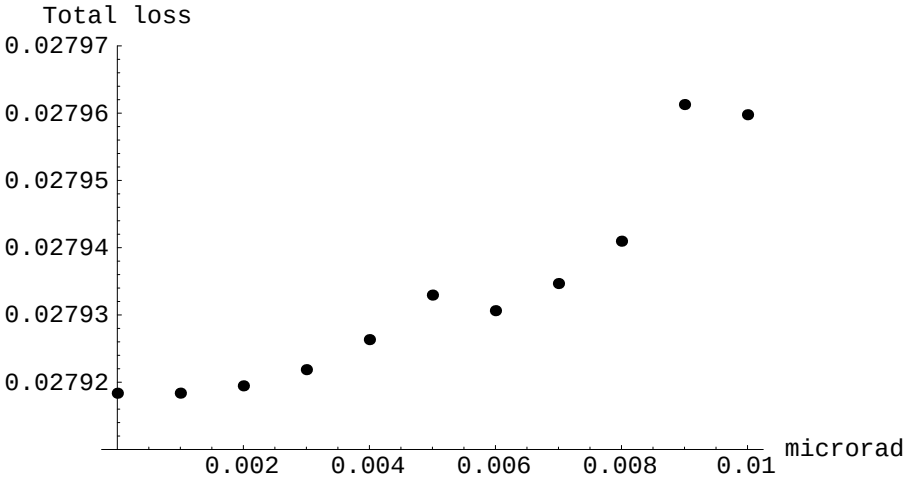

FIG. 19. The total loss is evaluated from the power driving the cavities minus the power detected at the antisymmetric port of the beamsplitter and the amount that goes back toward the laser reflected from the whole interferometer